

1 Basal expression of immune receptor genes requires low 2 levels of the phytohormone salicylic acid

3

4 Author list

5 Tijmen van Butselaar¹, Savani Silva¹, Dmitry Lapin¹, Iñigo Bañales¹, Sebastian Tonn¹, Chris van Schie²,
6 Guido Van den Ackerveken^{1*}

7 1 - Translational Plant Biology, Department of Biology, Institute of Environmental Biology,
8 Padualaan 8, 3584 CH Utrecht, The Netherlands

9 2 – Enza Zaden, Haling 1-E, 1602 DB, Enkhuizen, The Netherlands

10 * corresponding author

11

12 Abstract

13 The hormone salicylic acid (SA) plays a crucial role in plant immunity by activating responses that
14 arrest pathogen ingress. Since SA accumulation also penalizes growth, the question remains why
15 healthy plants synthesize this hormone. By overexpressing SA-inactivating hydroxylases in
16 *Arabidopsis thaliana*, we reveal that basal SA levels in unchallenged plants are needed for expression of
17 selected immune receptor and signaling genes, thereby enabling early pathogen detection and
18 activation of immunity.

19

20 Main text

21 Plants activate their immune response to biotrophic pathogens largely through the phytohormone
22 salicylic acid (SA)^{1,2}. This encompasses not only the transcriptional activation of defense genes but also
23 the repression of growth and development-related genes³ which translates into reduced plant
24 growth^{4,5}. This balance or so-called growth-immunity tradeoff must be well-controlled to circumvent
25 complete immunity-driven growth arrest^{4,5}. Therefore, plant SA responsiveness should be tightly
26 regulated through SA synthesis, catabolism, and signaling². In *Arabidopsis thaliana* (Arabidopsis
27 hereafter), SA catabolism is largely driven by the Fe(II) oxoglutarate-dependent oxygenases
28 DMR6/S5H (DOWNY MILDEW RESISTANT 6/SA 5-HYDROXYLASE) and its functionally redundant
29 paralog DLO1/S3H (DMR6-LIKE OXYGENASE 1/SA 3-HYDROXYLASE)⁶. DMR6 and DLO1 hydroxylate SA
30 to form 2,5-dihydroxybenzoic acid (2,5-DHBA) and 2,3-DHBA, respectively, which are rapidly
31 glucosylated and transported into plant vacuoles⁷⁻⁹. Reduced SA catabolism, as in *dmr6* and *dlo1* single
32 and double mutants, leads to increased SA levels, elevated expression of immunity-related genes, and
33 enhanced broad-spectrum resistance to biotrophic pathogens⁶⁻⁸. However, severe growth reduction is

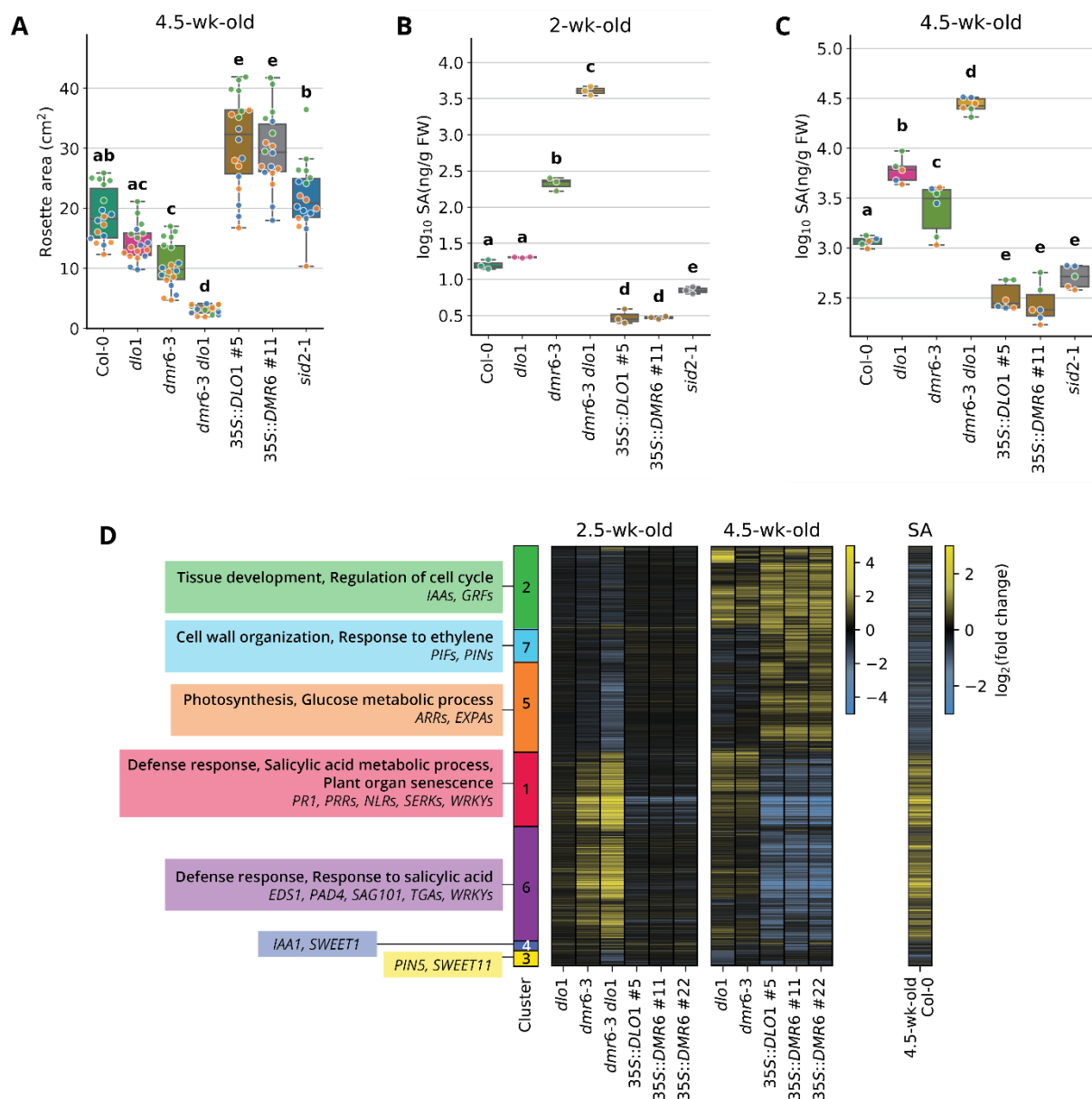
34 observed in the *dmr6 dlo1* double mutant, caused by hyperaccumulation of SA⁶. Conversely, plants
35 overexpressing *DMR6* or *DLO1* have lower SA levels, higher pathogen susceptibility, and increased
36 growth⁶⁻⁸. *dmr6*-based disease resistance is not only effective in Arabidopsis but also different crops¹⁰⁻
37 ¹⁷, demonstrating its potential for broad-spectrum resistance breeding.

38 Perturbation of *DMR6* and *DLO1* in Arabidopsis allows controlling basal SA levels in mutants and
39 overexpression lines and studying effects of SA on growth, immunity, gene expression, and other
40 responses without exogenous application of the hormone^{6,18}. Here, a comparison of transcriptomes
41 was carried out on Arabidopsis lines with perturbed expression of *DMR6* and *DLO1* (**Supplementary**
42 **Figure 1**). Overexpression of *DMR6* or *DLO1* in Arabidopsis Col-0 (hereafter Col) was associated with
43 increased rosette size of the 4.5-week-old plants and lower total SA levels in both 2- and 4.5-week-
44 old plants, in agreement with previous results^{6,8} (**Figure 1A-C**). Interestingly, the overexpression lines
45 were larger and had lower SA levels at two weeks than the *sid2-1* mutant which has strongly reduced
46 SA production (**Figure 1A-C**). Single *dmr6-3* (hereafter *dmr6*) and *dlo1* mutants grew smaller and had
47 increased SA levels compared to Col, whereas the *dmr6 dlo1* double mutant was severely reduced in
48 growth and accumulated high SA levels (**Figure 1A-C**). Due to severe leaf senescence^{6,8}, the 4.5-week-
49 old *dmr6 dlo1* mutant was excluded from the RNAseq analysis.

50 The largest transcriptome changes were detected in the 2.5-week-old *dmr6 dlo1* double mutant and
51 4.5-week-old *DMR6/DLO1* overexpression lines compared to Col (**Supplementary Figure 1A**). In total,
52 we found 6234 differentially expressed genes (DEG) between the Col control and mutants or
53 overexpression lines of the same age ($|\log_2FC| \geq 1$, FDR-adj. $p \leq 0.05$; **Figure 1D**, **Supplementary Figure**
54 **1B-C**). Hierarchical clustering grouped these genes into seven clusters (**Figure 1D**). Clusters 1 and 6
55 (1103 and 1705 DEG, respectively) contained genes upregulated in the 2.5-week-old *dmr6* single and
56 *dmr6 dlo1* double mutants but downregulated in 4.5-week-old *DMR6* or *DLO1* overexpression lines.
57 These clusters were enriched for SA and other immunity-related gene ontology (GO) terms (**Figure 1D**,
58 **Supplementary Figure 2**). In contrast, genes in clusters 2 (1217 DEG), 5 (1328), and 7 (504) were
59 downregulated in the 2.5-week-old *dmr6 dlo1* double mutant and upregulated in 4.5-week-old *DMR6*
60 or *DLO1* overexpression lines. They were enriched for GO terms associated with photosynthesis,
61 growth, and development (**Figure 1D**, **Supplementary Figure 2**). Similar to these GO enrichment
62 patterns, genes involved in immunity were also upregulated in tomato *dmr6* mutants¹² and the
63 Arabidopsis *dmr6-1* mutant¹⁹, while genes involved in photosynthesis, growth, and development were
64 downregulated in tomato *dmr6* mutants¹².

65 The highest number of DEG compared to Col was observed in 2.5-week-old *dmr6 dlo1* plants (3696
66 DEG) (**Figure 1B**). A stronger effect on the transcriptome was observed in young plants of the *dmr6*
67 single mutant than in older plants (666 and 83 DEG, respectively), whereas the opposite pattern was
68 observed in the *dlo1* mutant (8 and 851 DEG), suggesting that *DMR6* and *DLO1* are relatively more
69 important for SA catabolism in younger and older plants, respectively. The latter observation supports
70 the role of *DLO1* as a regulator of senescence induction⁸. This temporal effect of single mutants on the
71 transcriptome is also reflected in SA levels that are higher in *dmr6* than *dlo1* at 2 weeks but higher in
72 *dlo1* than *dmr6* at 4.5 weeks (**Figure 1B-C**)⁸. In the *DMR6* and *DLO1* overexpression lines, SA levels were

73 significantly lower in both 2- and 4.5-week-old plants compared to Col (**Figure 1B-C**). The
 74 overexpression lines had minor transcriptome changes relative to Col in 2.5-week-old plants, while
 75 they differed significantly at 4.5 weeks (2617 and 2774 in *35S::DMR6*, depending on the line, and 2895
 76 DEG in *35S::DLO1*; **Supplementary Figure 1B-C**). Together, these data suggest that reduced SA levels
 77 have an increasing effect on the transcriptome as the plants age. Although *DMR6* and *DLO1* produce
 78 different DHBAs, the transcriptome changes of 4.5-week-old *DMR6* and *DLO1* overexpression lines
 79 compared to Col were strongly correlated ($R^2=0.84$ to 0.91 , p -value < 0.001) (**Supplementary Figure 3A**)
 80 indicating that it is the removal of SA that drives transcriptome changes in these lines rather than the
 81 production of specific DHBAs. To independently validate that transcriptome changes in the tested
 82 genotypes are due to perturbed basal SA levels, we analyzed a published gene expression profile of SA-
 83 treated *Arabidopsis* leaves²⁰. It correlated positively with the transcriptome changes of the *dmr6 dlo1*
 84 mutant ($R^2=0.67$, p -value < 0.001) and negatively with that of the *DMR6/DLO1* overexpression lines
 85 ($R^2=-0.55$ to -0.64 , p -value < 0.001 ; **Figure 1D**, **Supplementary Figure 3B**).



87 **Figure 1. *DMR6/DLO1* perturbation influences Arabidopsis growth, SA levels, and transcriptomes. (A)**
88 Rosette area of 4.5-week-old plants with mutated or overexpressed *DMR6* and *DLO1* alongside controls
89 Col-0 and *sid2-1*. (B, C) Total SA levels in two (B) and 4.5 (C) week-old plants of indicated genotypes.
90 Data in A-C are from three independent experiments (indicated by differently colored dots in A and C;
91 in B, each dot represents an independent experiment). Different letters above the boxplots show
92 statistically significant differences between genotypes (two-way ANOVA (A, C) or one-way ANOVA (B)
93 followed by Tukey's post-hoc test, $p \leq 0.05$). Outliers were removed with interquartile range method
94 (IQR) in C. (D) Heatmap of \log_2 fold change values for the 6234 genes that were differentially expressed
95 ($|\log_2FC| \geq 1$, FDR-adj. $p \leq 0.05$) in *DMR6* and *DLO1* mutant or overexpression lines compared to the
96 age-matched wild-type. Selected GO terms enriched in seven clusters of co-expressed genes are listed
97 with example genes or gene families from each cluster. On the right is the RNAseq profile of Col leaves
98 24 hours after treatment with 0.5 mM SA²⁰.

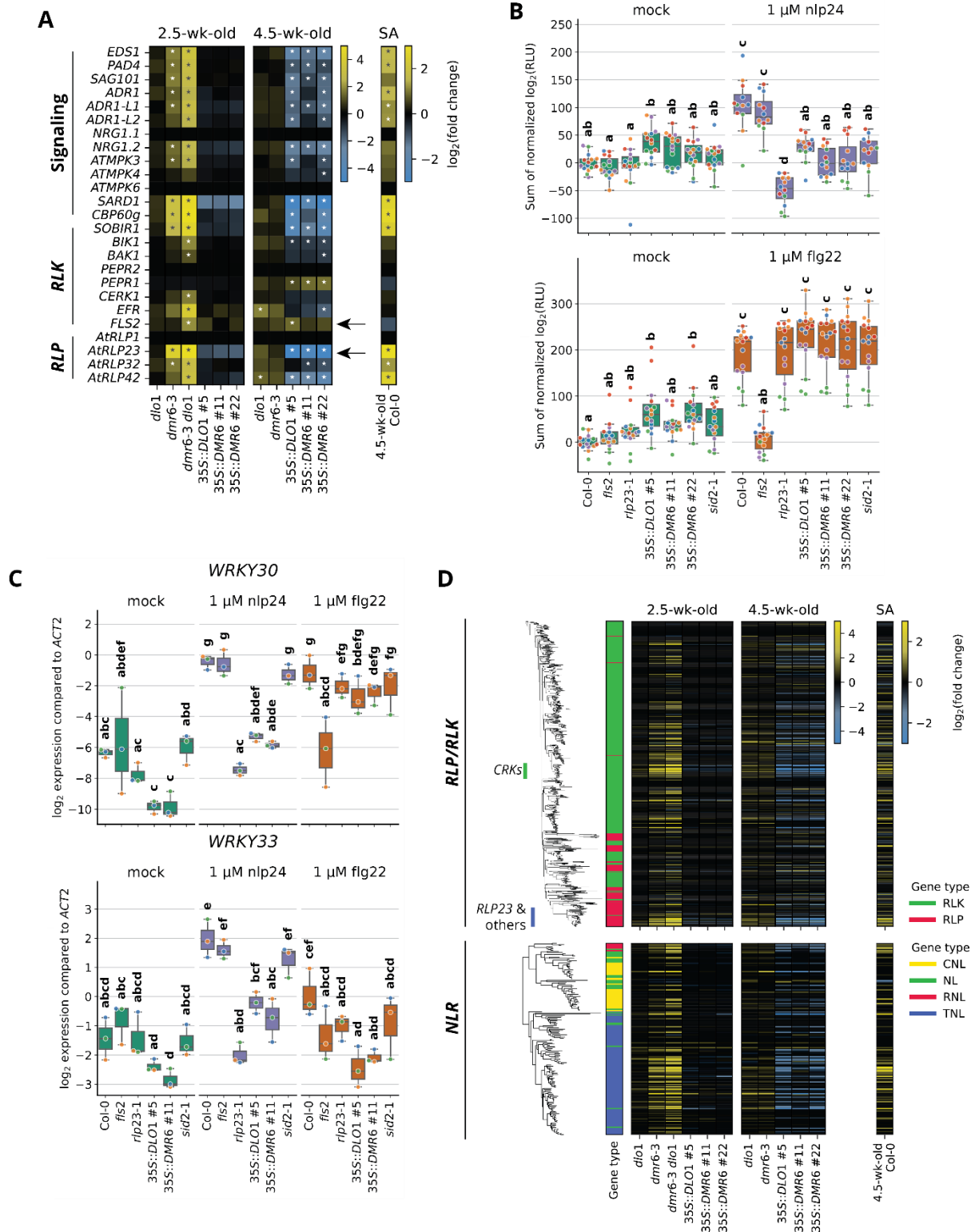
99 When inspecting the DEG clusters (**Figure 1D**) for known regulators of Arabidopsis immunity, we
100 noticed that 4.5-week-old *DMR6/DLO1* overexpression lines had reduced expression of genes involved
101 in pattern-triggered immunity (PTI) and effector-triggered immunity (ETI). Examples are *EDS1*
102 (*ENHANCED DISEASE SUSCEPTIBILITY 1*), its paralogous signaling partners *PAD4* (*PHYTOALEXIN*
103 *DEFICIENT 4*) and *SAG101* (*SENESCENCE-ASSOCIATED GENE 101*), genes encoding helper nucleotide-
104 binding leucine-rich repeat proteins (*NLRs*), selected immune receptors from the RLP class
105 (*RECEPTOR-LIKE PROTEINS*, including *RLP23*), and RLP co-receptor *SOBIR1* (*SUPPRESSOR OF BIR1 1*;
106 **Figure 2A**). On the other hand, expression of selected pattern recognition receptor genes from the RLK
107 (*RECEPTOR-LIKE KINASE*) class (e.g., *FLS2* (*FLAGELLIN-SENSITIVE 2*)) was not consistently suppressed
108 in the *DMR6/DLO1* overexpression lines (**Figure 2A**).

109 The altered expression of PTI-related genes prompted us to investigate the attenuation of early PTI
110 responses to the pathogen-associated molecular patterns (PAMPs) nlp24 and flg22 in the *DMR6/DLO1*
111 overexpression lines (**Figure 2B-C**). The nlp24-triggered ROS burst and the induction of *WRKY30* and
112 *WRKY33* were strongly reduced in *DMR6/DLO1* overexpression lines (**Figure 2B-C**). This fits the lower
113 expression of genes required for the nlp24-induced responses (*RLP23*, *SOBIR1*, *EDS1/PAD4/SAG101*, and
114 helper *NLRs*; **Figure 2A**). The flg22-triggered ROS burst and *WRKY30* and *WRKY33* induction were
115 unaffected in the *DMR6/DLO1* overexpression lines, aligning with the unaltered expression of RLKs
116 *FLS2* and *BAK1* (*BRI1-ASSOCIATED RECEPTOR KINASE 1*; **Figure 2A-C**). The single and double *dmr6* and
117 *dlo1* mutants behaved like Col in the tested outputs, suggesting that increasing SA levels does not
118 enhance early PTI responses (**Supplementary Figure 4**). To obtain additional evidence for the role of
119 basal SA levels and SA perception on early PTI responses, we tested the SA-deficient *sid2* mutant
120 (**Figure 1B-C**) and the SA-insensitive *npr1-1 npr4-4D* double mutant²¹. Both mutants showed reduced
121 nlp24-triggered ROS burst (**Figure 2B, Supplementary Figure 5**) confirming the dependency on SA for
122 nlp24 responsiveness.

123 To obtain a genome-wide view of the effects of *DMR6/DLO1* perturbation on immune receptor gene
124 expression, we analyzed the expression of Arabidopsis genes encoding for RLKs, RLPs, and *NLRs* in
125 *DMR6/DLO1* overexpression lines and mutants. We termed these genes SA-responsive if, compared to
126 the Col control, they were downregulated in the three *DMR6/DLO1* overexpression lines at 4.5 weeks

127 and upregulated in the *dmr6-3 dlo1* double mutant at 2.5 weeks ($|\log_2FC| \geq 1$, FDR-adj. $p \leq 0.05$). We found
128 that 120 *RLPs/RLKs* (14%) and 21 *NLRs* (13%) fell into this group. Notably, the phylogenetic clustering
129 of receptors did not separate SA-responsive genes from the rest (**Figure 2D**), indicating that the
130 dependency of their expression level on basal SA is not restricted to specific phylogenetic clades. We
131 further tested if SA-responsive receptor genes have enrichment of certain transcription factor binding
132 sites. Indeed, promoters of SA-responsive *RLP/RLK* and *NLR* genes showed specific enrichment of
133 WRKY transcription factor binding sites (**Supplementary Figure 6**), suggesting that WRKYs contribute
134 to SA dependence of the receptor gene expression.

135



136

137 **Figure 2. Reduction in the basal SA levels lowers the expression of selected immunity genes and**
 138 **associated PTI responses. (A) Expression of PTI-related genes, including signaling components and**
 139 **immune receptors in indicated genotypes. Asterisks denote the differential expression compared to the**
 140 **age-matched Col ($|\log_2FC| \geq 1$, FDR-adj. $p \leq 0.05$). (B) Reduced ROS burst in response to nlp24 (upper**
 141 **panel) but not to flg22 (lower) in the SA-depleted lines compared to Col-0. The *rlp23* and *fls2* mutants**
 142 **were negative controls for the nlp24 and flg22 treatments, respectively. RLU: relative luminescence**

143 units; mock: mQ. (C) Transcript levels of *WRKY30* and *WRKY33* in response to the *nlp24* and *flg22*
144 treatments. The *DMR6/DLO1* overexpression lines have *WRKY* gene induction to *nlp24*. *WRKY* transcript
145 levels were measured by qRT-PCR and receptor mutant lines *rlp23* and *fls2* were included as negative
146 controls. Plants in B and C were 4.5-week-old. Data displayed are derived from three independent
147 experiments, as indicated by differently colored dots. Different letters denote statistically different
148 groups from two-way ANOVA followed by Tukey's Post-Hoc test, $p \leq 0.05$. (D) Expression of 861 RLPs
149 and *RLKs* (top), and 166 *NLRs* (bottom) in *DMR6/DLO1* mutant and overexpression lines. Phylogenetic
150 analysis was performed on protein alignments. Abbreviations: CRK – cysteine-rich receptor-like
151 kinase, CNL, RNL and TNL – NLRs with coiled-coil, RPW8 (RESISTANCE TO POWDERY MILDEW 8),
152 and TIR (Toll/interleukin-1 receptor homology) domains, respectively.

153

154 So far, the role of SA in plant immunity was focused on defense signaling and senescence. Here, we
155 show that low basal levels of SA are important for the appropriate expression of genes encoding for
156 several groups of immunity-related RLPs and their immediate downstream signaling components.
157 Although plants grow better in the absence of basal SA, our results reveal a trade-off in pathogen
158 detection. This explains why low basal SA levels are needed to have a well-functioning plant immune
159 system.

160

161 Data availability

162 Raw read RNA-seq data have been deposited in the European Nucleotide Archive (ENA) database at
163 EMBL-EBI (<https://www.ebi.ac.uk/ena/>) under accession number PRJEB61019.

164

165 Acknowledgements

166 We would like to thank Nora Ludwig (deceased), Joyce Elberse, and Rob Schuurink for the
167 measurements of the hormone data in Figure 1B, part of which was published earlier in Zeilmaker, et
168 al. ⁶. This project was funded by Enza Zaden B.V. and Topsector Tuinbouw & Uitgangsmaterialen.
169

170 Author contributions

171 TvB and SS performed the RNAseq experiment; TvB, SS, DL, and GvdA analyzed RNAseq data; IB
172 conducted the phylogenetic analysis; TvB and CvS measured salicylic acid levels; TvB and DL performed
173 gene expression and ROS burst assays. TvB, DL, and GvdA wrote the manuscript with contributions
174 from all authors.

175

176 Authors declare no competing interests.

177 Material and Methods

178 Plant genotypes and growth conditions

179 Lines of *Arabidopsis thaliana* (L.) Heynh. Col-0 *dmr6-3*, *dlo1*, *dmr6-3 dlo1*, *35S:DMR6* and *35S:DLO1* were
180 previously described⁶. The Col-0 *npr1-1* and *npr1-1 npr4-4D* mutants (Ding, et al.²¹) were received from
181 Pingtao Ding (Leiden University, the Netherlands). Seeds were imbibed for four days at 4°C, either in
182 0.1% agarose and then transferred to soil (5:12 sand:soil mix, supplemented with half-strength
183 Hoagland solution, see Van Wees, et al.²²) or sown directly on soil. Plants were grown under short-day
184 (10h/14h light/dark, 21°C, 70% relative humidity, 100 µmol/m²/sec) conditions with regular watering
185 and a supplement of half-strength Hoagland solution once a week. During the first week of growth,
186 seeds were germinated under 100% RH.

187

188 RNA sequencing library preparation

189 Aerial parts of 2.5-week-old or the sixth leaf of 4.5-week-old plants were harvested and snap-frozen
190 in liquid nitrogen. RNA isolations and library preparations were performed according to Bjornson, et
191 al.²³ high-throughput RNA isolation and library prep protocols, with reagents from other suppliers
192 that are detailed below. Briefly, mRNA was enriched from crude cell lysate in two rounds using
193 biotinylated oligo-dT (IDT Europe) and streptavidin beads (New England Biolabs). RNA isolations were
194 performed in batches in a randomized order. Following cDNA synthesis and adapter ligation,
195 sequencing libraries were generated using indexed primers and enrichment primers (IDT Europe, see
196 Primer List) with Phusion HF polymerase (Thermo Fisher). Libraries were visually inspected on an
197 agarose gel before a double clean up with Ampure XP magnetic beads (Beckman). Library DNA quantity
198 was measured with SYBR Green (Thermo Fisher). Equalized amounts of libraries were pooled together
199 before a final Ampure XP cleanup. Libraries were sequenced at Useq (Utrecht, The Netherlands) on the
200 Illumina NextSeq2000 (P3 1x50nt) platform.

201

202 Transcriptome analysis

203 All sequencing data analyses on read files were performed in *slurm* workload manager on a local High-
204 Performance Computing Facility (University Medical Center Utrecht, The Netherlands). Illumina BCL
205 files were demultiplexed and converted to fastq format with *bcl2fastq* v2.20.0 (Illumina). Quality of
206 sequencing data was verified before and after trimming with *fastQC* v0.11.5 and *MultiQC* v1.5²⁴.
207 Trimming was performed with *trimmomatic* v0.39²⁵ using default settings and Truseq3-PE adapters.
208 Trimmed reads were pseudo-aligned to the TAIRv10 nuclear transcriptome with *kallisto* v0.46.1²⁶ using
209 a 21-mer index file. Only samples with least 5 million transcript-assigned reads were considered in
210 further analyses. For these samples, the reads per transcript were pooled per gene with *tximport* v1.24.0
211²⁷, and differential gene expression was performed with *deseq2* v1.36.0²⁸, using a DEG cutoff at $|\log_2FC|$
212 ≥ 1 , FDR-adj. $p \leq 0.05$.

213 Fold-change values were further processed in Python v3 using *pandas* 1.4.1 package for data handling
214 and *seaborn* 0.11.2 and *matplotlib* 3.5.1 packages for data visualization. Principal component analysis
215 (PCA) was performed with *scikit-learn* 0.24.2. UpSet plots²⁹ were generated with *upsetplot* 0.61 package
216 for Python using minimal subset size of 25 and minimal degrees of 2. Clustering of genes was
217 performed with hierarchical clustering from *SciPy* 1.7.1 *clusters.hierarchy* package, using *complete*
218 method and *correlation* metrics. Clusters were generated with *SciPy* 1.7.1 *hierarchy.cut_tree* method, and
219 the optimal *n* clusters for the dataset was determined after visual examination of the plots. Enrichment
220 of biological process gene ontology (GO) terms was performed in ClueGO v2.5.8 plugin for CytoScape
221³⁰. From the enrichment analysis we processed only the overview GO terms to minimize redundancy.
222 Pearson's correlation analyses were performed with *SciPy* 1.7.1. Enrichment of transcription factor
223 binding sites was conducted in *AME* from the *MEME* 5.4.1-suite³¹ on gene promoter sequences (1kb
224 upstream of translation start site) (TAIRv10). *AME* search was performed with motifs from DAP-seq
225 database³² and PBM database³³ and with an *E*-value threshold of 0.001.

226

227 Phylogenetic analyses

228 To find groups of sequence-related NLR proteins, the proteome of *A. thaliana* Col-0 (Araport11,
229 representative peptide sequences) was scanned against Pfam-A database (release 35.0, *pfam_scan.pl*
230 *-e_seq* 0.1 *-e_dom* 0.1), and NB-ARC domains (PF00931.25) of the corresponding 166 proteins were
231 extracted for phylogenetic analysis (Biopython v1.79). 92% of manually identified NLRs proteins were
232 supported by Araport11 annotation. Multiple sequence alignments (MSAs) were constructed with
233 MAFFT default parameters (v7.505, *--auto*)³⁴ and filtered for parsimony-informative sites. Alignment
234 columns with >60 % gaps were also removed (Clipkit v1.3.0, *-m kpic-gappy -g* 0.6). Filtered alignment
235 was inspected in the Wasabi MSA browser (<http://was.bi/>) prior to phylogeny reconstruction. The ML
236 trees were inferred with IQ-TREE (v.2.1.2, *-m* MFP *-B* 1000 *-alrt* 1000 *-T* auto)³⁵. The best-fit
237 substitution model for the data was determined by ModelFinder (JTT+F+R6)³⁶.

238 For the sequence-based grouping of Arabidopsis RLKs and RLPs, we used 695 RLKs and 175 RLPs
239 annotated in previous publications³⁷⁻³⁹ and from the RGAugury pipeline⁴⁰. Four sequences (AT1G16140,
240 AT4G21370, AT5G57670 and AT3G21960) were discarded since they were annotated as pseudogenes in
241 TAIR10.1. MSAs were constructed with MAFFT (v7.505, *--auto*) and filtered for parsimony-informative
242 sites. Alignment columns with >90 % gaps were also removed (Clipkit v1.3.0, *-m kpic-gappy -g* 0.6).
243 Filtered alignment was inspected in the Wasabi MSA browser (<http://was.bi/>) and the conserved region
244 was extracted for evolutionary inference (seqkit v2.3.0, region between 700:1379 columns).
245 AT5G49750 was removed from further analysis due to the lack of aligned positions in this area. The ML
246 trees were inferred with IQ-TREE (v.2.1.2, *-m* MFP *-B* 1000 *-alrt* 1000 *-T* auto). The best-fit
247 substitution model for the data was determined by ModelFinder (LG+F+R8). Resulting NB-ARC and
248 RLP/RLK trees were inspected and rooted in iTOL (v6)⁴¹.

249

250 Salicylic acid measurements

251 Total SA levels in two-week-old plants are from the experiment published in Zeilmaker, et al. ⁶ where
252 data for the *DMR6* and *DLO1* overexpression lines were unpublished. Total SA quantification on 4.5-
253 week-old plants was performed as follows. Aerial parts of plants were weighed to approximately 200
254 mg material, harvested in liquid nitrogen, and subsequently freeze-dried overnight. Samples were
255 homogenized with steel beads before extraction with 1 ml 80% ethanol 0.5% formic acid and 3 ppm 5-
256 fluorosalicylic acid (internal standard). Cell debris was spun down and supernatant was evaporated to
257 20% (water phase). The samples were hydrolyzed by addition of 25 μ l 5M HCl and incubation for 1 hour
258 at 90°C. Hydrolyzed samples were neutralized with 25 μ l 5M NaOH and re-extracted with 500 μ l ethyl
259 acetate. The organic phase was transferred to a new tube and 50 μ l 0.5% formic acid was added. The
260 sample was concentrated by evaporation to an approximate volume of 50 μ l, after which 50 μ l
261 methanol with 0.5% formic acid was added. Before LC/MS analysis, samples were spun to remove any
262 debris. For absolute quantitation of SA with a calibration/response-curve, SA was spiked into unrelated
263 Col-0 leaf samples before extraction in a concentration series. Samples were separated by UHPLC on a
264 Poroshell 120 column (2.1 x 100 mm, 1.9 micron pore) with pentafluorophenyl chemistry. Mobile phases
265 were: A) 5% methanol, 0.5% formic acid, 10 mM ammonium formate in MilliQ; B) 0.5% formic acid in
266 acetonitrile. Separation sequence was 20% B for 2.5', increasing to 50% B at 5' and increasing to 95%
267 B at 6'. Eluted metabolites were analyzed on an Agilent 6530 Q-TOF LC/MS in negative ion mode, with
268 dual EJS/ESI ionization. Quantitation was performed by quantifying peak areas from extracted ion
269 chromatograms of unfragmented parent ions (for SA m/z 137.023). Peak areas were corrected with
270 internal standard and sample fresh weight, and converted to absolute amounts using the external SA
271 spike-in calibration curve

272

273 Growth measurements

274 Rosette size was determined from topview images captured in a FluorCam 1300 system with Fluorcam
275 v10 software (Photo Systems Instruments, Czech Republic).

276

277 Measurement of the reactive oxygen species (ROS) burst

278 ROS burst assays were performed as in Johannndrees, et al. ⁴².

279

280 qPCR analysis of gene expression

281 Leaves of 4.5-week-old plants were syringe-infiltrated with mock (10 mM MgCl₂, 0.01% DMSO), 1 μ M
282 flg22, or 1 μ M nlp24. After 1 h of treatment, leaves were harvested, snap-frozen in liquid nitrogen, and
283 stored at -80°C. Tissue was homogenized in a TissueLyserII using 3mm glass beads. We used Spectrum
284 Plant Total RNA kit (Sigma Aldrich) to extract total RNA. cDNA was synthesized with RevertAid H-
285 minus reverse transcriptase (ThermoFisher) and oligo(dT)16 according to manufacturer's

286 instructions. qRT-PCR was performed with iTaq Universal SYBR Green Supermix (Bio-Rad) according
287 to manufacturer's instructions on a ViiA 7 system (ThermoFisher). Primers are listed in
288 **Supplementary Table 1**. qRT-PCR analysis was performed by averaging Ct values of technical replicates
289 and calculating Δ Ct per sample by subtracting Ct of target gene from the Ct of the *ACTIN2* gene
290 (*AT3G18780*). Statistics and visualization was based on these Δ Ct values.

291

292 Data analysis and visualization

293 All data analyses were performed in Spyder IE for Python v3 using *pandas* 1.4.1 package for data
294 handling and *seaborn* 0.11.2 and *matplotlib* 3.5.1 packages for data visualization. Datasets were verified
295 to have a normal distribution with Shapiro-Wilk test of normality ($p > 0.05$), but were allowed to have
296 unequal variances (Bartlett's test). Shapiro-Wilk, Bartlett's tests, Student's t-tests, Pearson's
297 correlation analysis were performed with *SciPy* 1.7.1. ANOVA, Tukey's Post-Hoc analyses, and FDR
298 (Benjamini-Hochberg) multiple test correction were performed with *statsmodels* 0.12.2. Significance
299 groups were determined based on Piepho⁴³ implemented in a Python script.

300

301 References

- 302 1 Pieterse, C. M., Leon-Reyes, A., Van der Ent, S. & Van Wees, S. C. Networking by small-molecule
303 hormones in plant immunity. *Nat Chem Biol* 5, 308-316 (2009).
304 <https://doi.org/10.1038/nchembio.164>
- 305 2 Ding, P. & Ding, Y. Stories of Salicylic Acid: A Plant Defense Hormone. *Trends Plant Sci* 25, 549-
306 565 (2020). <https://doi.org/10.1016/j.tplants.2020.01.004>
- 307 3 Hickman, R. *et al.* Transcriptional Dynamics of the Salicylic Acid Response and its Interplay
308 with the Jasmonic Acid Pathway. *bioRxiv*, 742742 (2019). <https://doi.org/10.1101/742742>
- 309 4 Huot, B., Yao, J., Montgomery, B. L. & He, S. Growth-Defense Tradeoffs in Plants: A Balancing
310 Act to Optimize Fitness. *Mol Plant* 7, 1267-1287 (2014). <https://doi.org/10.1093/mp/ssu049>
- 311 5 van Butselaar, T. & Van den Ackerveken, G. Salicylic Acid Steers the Growth-Immunity
312 Tradeoff. *Trends Plant Sci* 25, 566-576 (2020). <https://doi.org/10.1016/j.tplants.2020.02.002>
- 313 6 Zeilmaker, T. *et al.* DOWNY MILDEW RESISTANT 6 and DMR6-LIKE OXYGENASE 1 are partially
314 redundant but distinct suppressors of immunity in Arabidopsis. *The Plant Journal* 81, 210-222
315 (2015). <https://doi.org/10.1111/tpj.12719>
- 316 7 Zhang, K., Halitschke, R., Yin, C., Liu, C. J. & Gan, S. S. Salicylic acid 3-hydroxylase regulates
317 Arabidopsis leaf longevity by mediating salicylic acid catabolism. *Proc Natl Acad Sci* 110, 14807-
318 14812 (2013). <https://doi.org/10.1073/pnas.1302702110>
- 319 8 Zhang, Y. *et al.* S5H/DMR6 Encodes a Salicylic Acid 5-Hydroxylase That Fine-Tunes Salicylic
320 Acid Homeostasis. *Plant Physiol* 175, 1082-1093 (2017). <https://doi.org/10.1104/pp.17.00695>
- 321 9 Bartsch, M. *et al.* Accumulation of isochorismate-derived 2,3-dihydroxybenzoic 3-O-beta-D-
322 xyloside in arabidopsis resistance to pathogens and ageing of leaves. *J Biol Chem* 285, 25654-
323 25665 (2010). <https://doi.org/10.1074/jbc.M109.092569>
- 324 10 Tripathi, J. N., Ntui, V. O., Shah, T. & Tripathi, L. CRISPR/Cas9-mediated editing of DMR6
325 orthologue in banana (*Musa spp.*) confers enhanced resistance to bacterial disease. *Plant*
326 *Biotechnol J* 19, 1291-1293 (2021). <https://doi.org/10.1111/pbi.13614>
- 327 11 Kieu, N. P., Lenman, M., Wang, E. S., Petersen, B. L. & Andreasson, E. Mutations introduced in
328 susceptibility genes through CRISPR/Cas9 genome editing confer increased late blight
329 resistance in potatoes. *Sci Rep* 11, 4487 (2021). <https://doi.org/10.1038/s41598-021-83972-w>
- 330 12 Thomazella, D. P. T. *et al.* Loss of function of a DMR6 ortholog in tomato confers broad-
331 spectrum disease resistance. *Proc Natl Acad Sci* 118, e2026152118 (2021).
332 <https://doi.org/10.1073/pnas.2026152118>

- 333 13 Pirrello, C. *et al.* Grapevine DMR6-1 Is a Candidate Gene for Susceptibility to Downy Mildew.
334 *Biomolecules* **12** (2022). <https://doi.org:10.3390/biom12020182>
- 335 14 Parajuli, S. *et al.* Editing the CsDMR6 gene in citrus results in resistance to the bacterial disease
336 citrus canker. *Hortic Res* **9**, uhac082 (2022). <https://doi.org:10.1093/hr/uhac082>
- 337 15 Low, Y. C., Lawton, M. A. & Di, R. Validation of barley 2OGO gene as a functional orthologue of
338 Arabidopsis DMR6 gene in Fusarium head blight susceptibility. *Sci Rep* **10**, 9935 (2020).
339 <https://doi.org:10.1038/s41598-020-67006-5>
- 340 16 Liang, B. *et al.* Salicylic Acid Is Required for Broad-Spectrum Disease Resistance in Rice. *Int J*
341 *Mol Sci* **23** (2022). <https://doi.org:10.3390/ijms23031354>
- 342 17 Hasley, J. A. R., Navet, N. & Tian, M. CRISPR/Cas9-mediated mutagenesis of sweet basil
343 candidate susceptibility gene ObDMR6 enhances downy mildew resistance. *PLoS One* **16**,
344 e0253245 (2021). <https://doi.org:10.1371/journal.pone.0253245>
- 345 18 Cai, Z. *et al.* Generation of the salicylic acid deficient Arabidopsis via a synthetic salicylic acid
346 hydroxylase expression cassette. *Plant Methods* **18**, 89 (2022). <https://doi.org:10.1186/s13007-022-00922-x>
- 347
348 19 van Damme, M., Huibers, R. P., Elberse, J. & Van den Ackerveken, G. Arabidopsis DMR6 encodes
349 a putative 2OG-Fe(II) oxygenase that is defense-associated but required for susceptibility to
350 downy mildew. *The Plant Journal* **54**, 785-793 (2008). <https://doi.org:10.1111/j.1365-313X.2008.03427.x>
- 351
352 20 Furniss, J. J. *et al.* Proteasome-associated HECT-type ubiquitin ligase activity is required for
353 plant immunity. *PLoS Pathog* **14**, e1007447 (2018).
354 <https://doi.org:10.1371/journal.ppat.1007447>
- 355 21 Ding, Y. *et al.* Opposite Roles of Salicylic Acid Receptors NPR1 and NPR3/NPR4 in
356 Transcriptional Regulation of Plant Immunity. *Cell* **173**, 1454-1467 (2018).
357 <https://doi.org:10.1016/j.cell.2018.03.044>
- 358 22 Van Wees, S. C., Van Pelt, J. A., Bakker, P. A. & Pieterse, C. M. J. Bioassays for assessing
359 jasmonate-dependent defenses triggered by pathogens, herbivorous insects, or beneficial
360 rhizobacteria. *Methods Mol Biol* **1011**, 35-49 (2013). https://doi.org:10.1007/978-1-62703-414-2_4
- 361
362 23 Bjornson, M., Kajala, K., Zipfel, C. & Ding, P. Low-cost and High-throughput RNA-seq Library
363 Preparation for Illumina Sequencing from Plant Tissue. *Bio Protoc* **10**, e3799 (2020).
364 <https://doi.org:10.21769/BioProtoc.3799>
- 365 24 Ewels, P., Magnusson, M., Lundin, S. & Kaller, M. MultiQC: summarize analysis results for
366 multiple tools and samples in a single report. *Bioinformatics* **32**, 3047-3048 (2016).
367 <https://doi.org:10.1093/bioinformatics/btw354>
- 368 25 Bolger, A. M., Lohse, M. & Usadel, B. Trimmomatic: a flexible trimmer for Illumina sequence
369 data. *Bioinformatics* **30**, 2114-2120 (2014). <https://doi.org:10.1093/bioinformatics/btu170>
- 370 26 Bray, N. L., Pimentel, H., Melsted, P. & Pachter, L. Near-optimal probabilistic RNA-seq
371 quantification. *Nat Biotechnol* **34**, 525-527 (2016). <https://doi.org:10.1038/nbt.3519>
- 372 27 Sonesson, C., Love, M. I. & Robinson, M. D. Differential analyses for RNA-seq: transcript-level
373 estimates improve gene-level inferences. *F1000Research* **4**, 1521 (2015).
374 <https://doi.org:10.12688/f1000research.7563.1>
- 375 28 Love, M. I., Huber, W. & Anders, S. Moderated estimation of fold change and dispersion for
376 RNA-seq data with DESeq2. *Genome Biol* **15**, 550 (2014). <https://doi.org:10.1186/s13059-014-0550-8>
- 377
378 29 Lex, A., Gehlenborg, N., Strobel, H., Vuillemot, R. & Pfister, H. UpSet: Visualization of
379 Intersecting Sets. *IEEE Trans Vis Comput Graph* **20**, 1983-1992 (2014).
380 <https://doi.org:10.1109/TVCG.2014.2346248>
- 381 30 Bindea, G. *et al.* ClueGO: a Cytoscape plug-in to decipher functionally grouped gene ontology
382 and pathway annotation networks. *Bioinformatics* **25**, 1091-1093 (2009).
383 <https://doi.org:10.1093/bioinformatics/btp101>
- 384 31 McLeay, R. C. & Bailey, T. L. Motif Enrichment Analysis: a unified framework and an evaluation
385 on ChIP data. *BMC Bioinformatics* **11**, 165 (2010). <https://doi.org:10.1186/1471-2105-11-165>
- 386 32 O'Malley, R. C. *et al.* Cistrome and Epicistrome Features Shape the Regulatory DNA Landscape.
387 *Cell* **165**, 1280-1292 (2016). <https://doi.org:10.1016/j.cell.2016.04.038>
- 388 33 Franco-Zorrilla, J. M. *et al.* DNA-binding specificities of plant transcription factors and their
389 potential to define target genes. *Proc Natl Acad Sci* **111**, 2367-2372 (2014).
390 <https://doi.org:10.1073/pnas.1316278111>
- 391 34 Katoh, K., Misawa, K., Kuma, K. & Miyata, T. MAFFT: a novel method for rapid multiple
392 sequence alignment based on fast Fourier transform. *Nucleic Acids Res* **30**, 3059-3066 (2002).
393 <https://doi.org:10.1093/nar/gk436>

- 394 35 Minh, B. Q. *et al.* IQ-TREE 2: New Models and Efficient Methods for Phylogenetic Inference in
395 the Genomic Era. *Mol Biol Evol* **37**, 1530–1534 (2020). <https://doi.org/10.1093/molbev/msaa015>
396 36 Kalyaanamoorthy, S., Minh, B. Q., Wong, T. K. F., von Haeseler, A. & Jermiin, L. S. ModelFinder:
397 fast model selection for accurate phylogenetic estimates. *Nat Methods* **14**, 587–589 (2017).
398 <https://doi.org/10.1038/nmeth.4285>
399 37 Shiu, S. H. *et al.* Comparative analysis of the receptor-like kinase family in Arabidopsis and rice.
400 *Plant Cell* **16**, 1220–1234 (2004). <https://doi.org/10.1105/tpc.020834>
401 38 Restrepo-Montoya, D., Brueggeman, R., McClean, P. E. & Osorno, J. M. Computational
402 identification of receptor-like kinases "RLK" and receptor-like proteins "RLP" in legumes.
403 *BMC Genomics* **21**, 459 (2020). <https://doi.org/10.1186/s12864-020-06844-z>
404 39 Wang, G. *et al.* A genome-wide functional investigation into the roles of receptor-like proteins
405 in Arabidopsis. *Plant Physiol* **147**, 503–517 (2008). <https://doi.org/10.1104/pp.108.119487>
406 40 Li, P. *et al.* RGAugury: a pipeline for genome-wide prediction of resistance gene analogs (RGAs)
407 in plants. *BMC Genomics* **17**, 852 (2016). <https://doi.org/10.1186/s12864-016-3197-x>
408 41 Letunic, I. & Bork, P. Interactive Tree Of Life (iTOL) v5: an online tool for phylogenetic tree
409 display and annotation. *Nucleic Acids Res* **49**, W293–W296 (2021).
410 <https://doi.org/10.1093/nar/gkab301>
411 42 Johannndrees, O. *et al.* Variation in plant Toll/Interleukin-1 receptor domain protein
412 dependence on ENHANCED DISEASE SUSCEPTIBILITY 1. *Plant Physiol*, kiac480 (2022).
413 <https://doi.org/10.1093/plphys/kiac480>
414 43 Piepho, H.-P. An Algorithm for a Letter-Based Representation of All-Pairwise Comparisons.
415 *Journal of Computational and Graphical Statistics* **13**, 456–466 (2004).
416 <https://doi.org/10.1198/1061860043515>